Sensors and Materials, Vol. 33, No. 2 (2021) 541–554
MYU Tokyo

S & M 2474

Design and Application of Flexible Piezoelectric Organic Thin-film Transistor Sensing System

Yajiang Ding, Cheng Ji, Junhui Yang, Meng Xu, and Xiaohong Yang*

Beijing Institute of Special Electromechanical Technology, Beijing 100012, China

(Received September 23, 2020; accepted November 25, 2020)

Keywords: electrohydrodynamic direct-writing technology, ultrastretchable piezoelectric sensor, organic thin-film transistor, piezoelectric sensor, flexible piezoelectric OTFT sensor system

Flexible sensor systems have paved the way for development in the field of next-generation flexible electronics, as traditional micro/nanoscale manufacturing processes cannot meet the requirements of industrial production for particular structures and materials. In this paper, a high-performance, flexible, and ultrastretchable piezoelectric sensor is realized with the help of an electrohydrodynamic direct-writing technology. The sensor is used directly for monitoring human body movements, breathing, and other actions, and outputs a stable and consistent electrical signal. At the same time, the design and application of a flexible piezoelectric organic thin-film transistor (OTFT) sensor system are realized using a flexible OTFT device prepared using an electrohydrodynamic direct-writing technology. The system produces a signal with very high magnification (1000 times) compared with the original signal and solves the conventional problems of a weak output signal and susceptibility to interference. The flexible piezoelectric OTFT sensor system can thus effectively monitor the speed of a human joint movement, stride frequency, and so forth, demonstrating its practical applicability.

1. Introduction

The prosperity in the flexible electronics industry has necessitated the urgent development of flexible devices in wearable applications.[1–4] Wearable electronic devices have two important requirements: (i) relatively high flexibility and stretchability, and (ii) extremely high sensitivity. High flexibility and stretchability are necessary to sustain the deformation caused by a human body movement without any negative effect on original electrical properties.[5,6] Extremely high sensitivity is required for the output signal to be captured and processed by a traditional signal acquisition circuit to guarantee the accurate analysis of the electric signal by the sensing system along with a precise detection function.

The electric properties of implantable energy acquirers and sensors in flexible electronic devices depend mainly on piezoelectric materials, which achieve a real-time feedback of electric signals through the responses of the functional layer to the detectable quantity.

*Corresponding author: e-mail: zhuyange123@qq.com
https://doi.org/10.18494/SAM.2021.3094

ISSN 0914-4935

Typical piezoelectric materials are ZnO quartz crystal, lead zirconate titanate (PZT) piezoceramics, and polyvinylidene difluoride (PVDF) piezoelectric polymer. As compared with inorganic piezoelectric materials such as ZnO and PZT, PVDF not only exhibits superior piezoelectric properties but also has advantages such as low cost and flexibility, contributing to its unparalleled preference in flexible piezoelectric devices. On the one hand, PVDF, a kind of organic polymer, can be produced as a homogeneous stable solution, which in conjunction with electrospinning can be used for the efficient preparation of a PVDF fiber membrane. On the other hand, during electrohydrodynamic printing, the electric force exerted by the high-voltage electric field on PVDF materials, together with the mechanical strain generated by the movement of the basal plate, facilitates the conversion of α crystal without piezoelectricity into piezoelectric β crystal. Consequently, piezoelectric fiber arrays can be obtained with a high conversion rate without post-polarization treatment. A series of studies have been performed on the preparation of flexible PVDF sensors[7–9] or energy acquirers[10–13] through electrospinning. However, the flexible piezoelectric devices currently available can sustain only small bending or stretching. The capacity to respond to only small strains is hindering actual applications as the demand for large-deformation applications is increasing continuously. Furthermore, the signal perceived directly by the flexible module is rather weak, and the generated current or voltage electric signal can hardly be captured directly by traditional circuits, making them infeasible for convenient use in real-time acquisition and processing. Hence, an organic thin-film transistor (OTFT) can be added at the end of the sensor module to amplify the electric signal, facilitating real-time signal acquisition and processing. Such a design achieves better sensor performance with a lower hardware cost. The establishment of such sensing systems has been the focus of multiple investigations, in which a flexible sensor was connected to a thin-film transistor as an amplifier, enabling the efficient acquisition of weak signals.[14–18] Rogers *et al*.[17] carried out the detection of a human pulse wave with the combination of a PZT sensor and transistors. Someya *et al*.[14] connected a dinaphtho[2,3-b:2′,3′-f] thieno [3,2-b] thiophene (DNTT) transistor and a resistance-type tactile sensor to detect a large-area pressure distribution. Someya *et al*.[18] measured the tissue temperature distribution inside a mouse as reference information for wound healing by using a temperature sensor array and an OTFT array. In the investigations mentioned above, in addition to the different dimensions, the manufacturing process was also different for the sensor and amplifier modules, contributing to difficulties in integration. Therefore, a new process is required for the preparation and integration of high-performance sensors and transistors.

In this paper, the buckling phenomenon from the impact on a basal plate of a fluid issued during electrohydrodynamic printing is incorporated into a controllable electrohydrodynamic direct-writing technology to prepare fibers with various structures. This technology is used for the preparation of flexible, high-performance OTFTs as well as ultrastretchable and ultrasensitive sensors. We integrate the two devices into a compact sensing system for the conversion of a weak electric signal, generated as a response to a human body movement, into a strong electric signal compatible with traditional acquisition circuits. This study serves as technological guidance for applications of wearable devices.

2. Preparation of Ultrastretched Piezoelectric Sensor and Detection of Human Body Movements

2.1 Structure of ultrastretchable piezoelectric sensor

For a mature, flexible electronic system, a flexible sensing module is an indispensable component. The sensors in flexible sensing systems mainly include force/displacement sensors, physical signal sensors for electrocardiography, myoelectricity, or pulse, and optical/thermal sensors. In order to obtain a precise and stable feedback signal, the macroflexibility of devices is achieved using a traditional electronic sensor module in conjunction with a deformable interconnection structure. However, this structure has several disadvantages, such as a large number of requirements for manufacturing, limited deformation, and a high risk of rupture failure in hard sensors. Thus, it is necessary to propose a simple and efficient preparation technology for deformable ultrasensitive sensors.

The overall structure of an ultrastretchable piezoelectric sensor is illustrated in Fig. 1(a). Under an external mechanical force, the generated strain in an in-plane buckled PVDF fiber with a two-layered corrugated structure leads to the conversion of mechanical energy into electrical energy, and the electric energy output is implemented through an accumulated

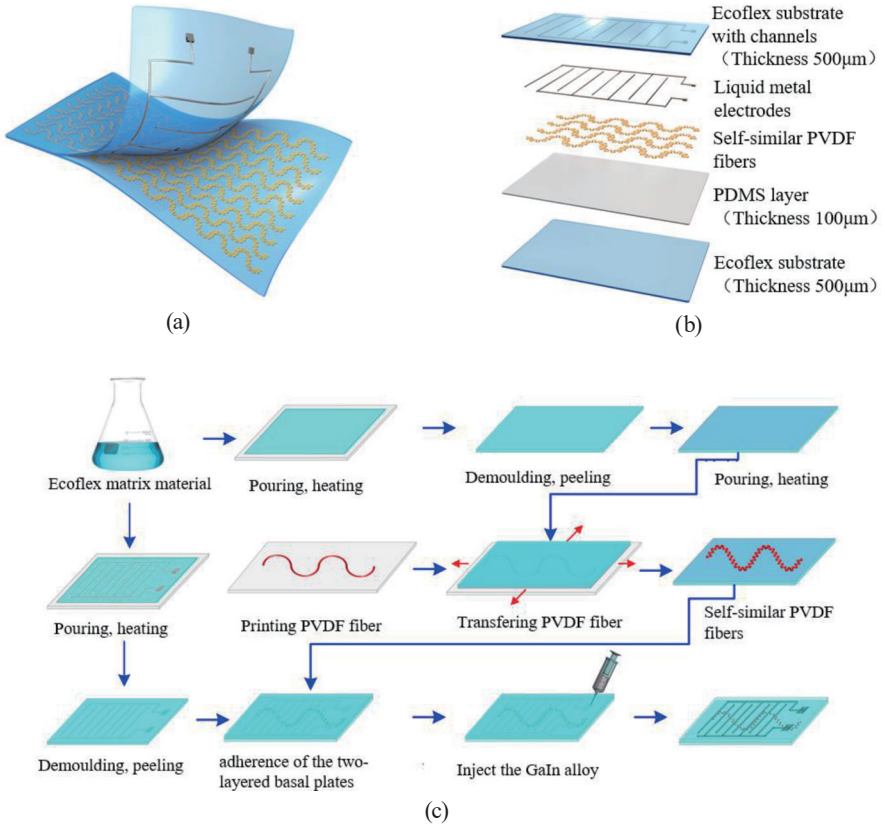

Fig. 1. (Color online) (a) Illustration of ultrastretchable sensor, (b) illustration of sensor structure, and (c) preparation of sensor.

voltage or current by coplanar electrodes. Figure 1(b) illustrates the five layers of our proposed piezoelectric sensor. The top Ecoflex membrane that acts as a sealing and supporting device is equipped with a microchannel and mainly serves as the reservoir for liquid metal electrodes. The PDMS layer is mainly responsible for the enhanced adhesion between the solidified Ecoflex layers, guaranteeing the complete sealing of the liquid metal inside the channel. The metal layer of GaIn alloy is a liquid at room temperature, and its capability to maintain the conducting state under the stretching or bending of the devices allows the persistent transmission of the electric energy from the PVDF. The PVDF fiber layer, organized as a two-layered corrugated structure, behaves as a functional layer to convert the external mechanical energy into electric energy. The fiber with a two-layered structure enables ultrastretchability, with stable piezoelectric properties retained after biaxial stretching above 100%. The bottom Ecoflex layer serves as the sealing and supporting layer, which also protects the internal structure from damage due to repeated stretching. Figure 1(c) provides details of the preparation method for a specific ultrastretchable piezoelectric sensor structure based on the PVDF fibers mentioned above.

Firstly, a uniform solution is obtained by thoroughly stirring a mixture of Ecoflex matrix material and curing agent with a ratio of 1:1, and the bubbles in the solution are removed by evacuation. Secondly, the Ecoflex solution is poured into a premachined metal die, ensuring that the die is completely filled, then heated in an oven at 60 °C for 10 min under atmospheric pressure to solidify the Ecoflex. Thirdly, controlled electrohydrodynamic printing is utilized to prepare an array of corrugated PVDF fibers on a silicon wafer. Then, biaxial stretching is imposed on the patternless Ecoflex membrane to transfer the PVDF, prepared on the silicon wafer, onto the Ecoflex. The PDMS solution is spread uniformly on the convex part of the patterned Ecoflex basal plate, which is assembled with the fiber-printed Ecoflex membrane basal plate. Then, the assembly is heated in an oven at 60 °C for 10–15 min under atmospheric pressure to adhere the two-layered basal plates. Finally, an injector is used to inject GaIn alloy into a microchannel with a depth of 400 μm. (The details of the electrohydrodynamic printing process (e.g., materials and equipment) are given in Supplement A.)

The thus manufactured ultrastretchable piezoelectric sensor is shown in Fig. 2(a). The functional module is rectangular with a dimension of approximately 80 mm and the

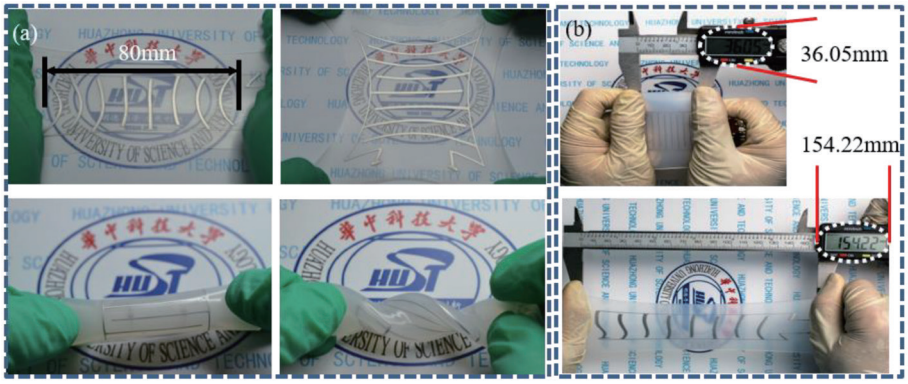

Fig. 2. (Color online) (a) Schematic view of ultrastretchable energy acquirer in original state and after unilateral stretching, biaxial stretching, and curling and distortion. (b) View of sensor in original and ultimately stretched states.

piezoelectric area only covers the coplanar electrode area of 35 × 25 mm^2. The outer membrane basal plate provides a convenient grip during testing. Owing to the large deformation bearing capacity of the device components, including the Ecoflex, PVDF fibers, and liquid metal, the whole device exhibits superior deformability and stretchability. Figure 2(a) shows the stable deformation of the device under unilateral stretching, biaxial stretching, and curling and distortion. With the removal of external forces, the device regains its original state while sustaining repeated stretching for thousands of times without rupture. Figure 2(b) shows a comparison between the original and stretched states of the piezoelectric sensor. The device originally has a length of 36.05 mm but can be horizontally stretched to a maximum length of 154.22 mm without damage to the device structure, corresponding to a deformability of 328%. To the best of the authors' knowledge, such an extremely high deformability significantly exceeds those of other currently available stretchable piezoelectric sensors.

2.2 Quantification of basic performance of ultrastretchable piezoelectric sensor and its performance in monitoring human body movement

For the application of the proposed ultrastretchable sensor to monitor human body movements, a mechanical motion apparatus is used to model a practical situation and to verify the basic sensing function and related principle. After the verification, the sensors are positioned on a human body to monitor its movement.

First, the as-prepared PVDF piezoelectric sensor is fixed firmly by mechanical gripping on a self-designed machine capable of producing stretching motion, and two shielded conductors are inserted at the two ends of the liquid metal electrode. Subsequently, the other end of each shielded conductor is connected to a thin metal by soldering. A 4200-SCS semiconductor tester from Keithley is used for the real-time monitoring of the output voltage–current signal from the piezoelectric sensor. The displacement and moving speed of the stretching machine can be adjusted by using software, and hence the flexible device can repeat a sequence of stretching and distortion. The deformation of the device leads to strain in the PVDF fibers, and the generated electric signal is displayed by a semiconductor tester. Figure 3 shows the output voltage–current signal under various operating conditions. The variation in output signal intensity clearly shows stability and regularity. Furthermore, owing to the piezoelectricity of the PVDF, the produced voltage–current signal is synchronous with a phase difference of 180°. Hence, only the produced current signal is selected for the statistical analysis of the piezoelectricity of the device. (The detailed descriptions of some basic principles of the PVDF are explained in Supplement B.)

Figures 3(a) and 3(b) present the output current signal under the stretching of the device along and perpendicular to the fiber orientation, respectively, with a constant magnitude of 120% and various stretching speeds. When the stretching direction is the same as the orientation of the PVDF fibers, as shown in Fig. 3(a), the currents produced by the device are 3, 6, 12, and 18 nA in response to stretching speeds of 20, 40, 80, and 160 mm/s, respectively. When the stretching direction is perpendicular to the PVDF fiber orientation, the produced currents are 1.5, 2.5, 4, and 6 nA, respectively, for the same stretching speeds. In the second

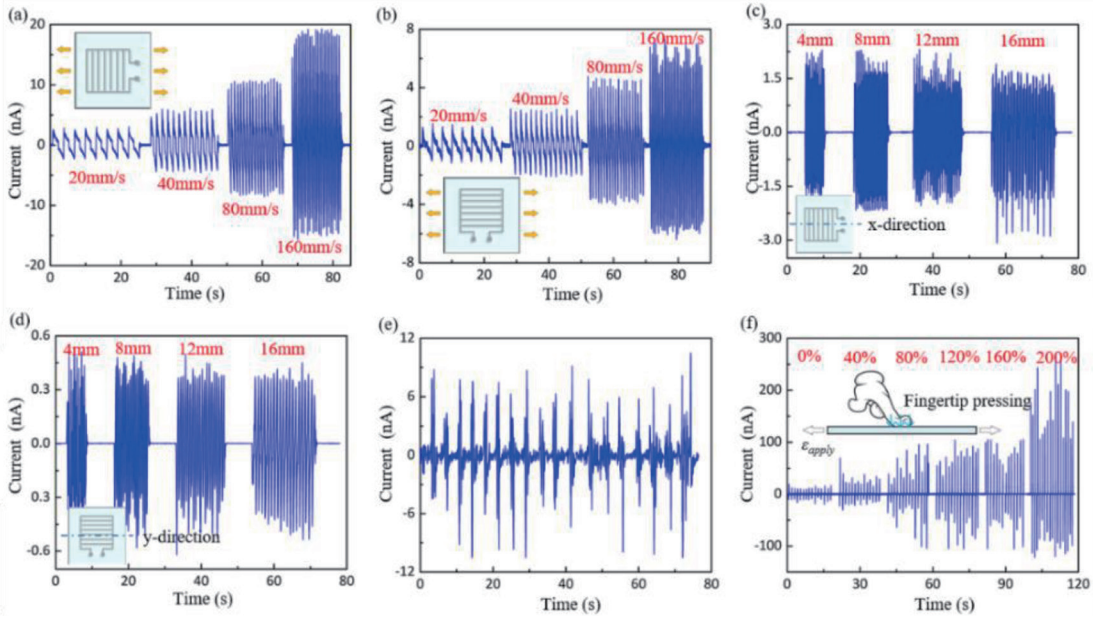

Fig. 3. (Color online) Electric properties of ultrastretchable piezoelectric sensor. Current response to (a) stretching along fiber orientation at various speeds, (b) stretching along direction perpendicular to fiber orientation at various speeds, (c) bending along fiber orientation with various bending magnitudes, (d) bending along direction perpendicular to fiber orientation with various bending magnitudes, (e) torsion imposed on device, and (f) fingertip pressing along fiber orientation with various amounts of stretching.

case, the output current increases almost proportionally with the stretching speed. The constant of proportionality is larger in the case of Fig. 3(a), where the stretching direction is the same as the fiber orientation, than in the case of Fig. 3(b), where the stretching direction is perpendicular to the fiber orientation. This is because of the horizontal piezoelectric coefficient being larger than the perpendicular coefficient. The ultrasensitive sensor could sustain bending deformation along two different directions as a consequence of the flexibility of the Ecoflex basal plate. Figures 3(c)–3(d) present the current signal produced by the device as a result of bending with various magnitudes at a constant bending speed of 40 mm/s along the same two directions. When the device is bent in the direction of the fiber orientation, the output signal remains unchanged at 1.5 nA, independent of the bending magnitude. When the device is bent in the direction perpendicular to the fiber orientation, the output signal remains unchanged at 0.4 nA, also independent of the bending magnitude. Furthermore, the fiber strain in such cases is negligible, and thus the produced current is rather weak. Figure 3(e) presents the electric signal of the energy acquirer produced under consecutive distortions. Since the distortions are imposed manually, both their amplitude and frequency exhibit marked nonuniformity. Nevertheless, the evident piezoelectric effect resulting from the distorted device can be identified. Figure 3(f) illustrates the output current from pressing a fingertip under different stretching rates. For the same magnitude of the pressing force, the output signal increases linearly from 20 to 200 nA as the stretching rate increases from 0 to 200%. This indicates that a relatively high stretching rate can increase the piezoelectric conversion efficiency. The relatively low consistency of the output

signal is ascribed to the inaccurate control of the manually imposed pressing force with low stability.

Figure 4 shows the output electric signal of the device when attached to different moving parts of the human body. When the device is fastened to the wrist, elbow, and knee, it generates a stable output current in response to the motion of the part with a normal speed and amplitude, as respectively shown in Figs. 4(a)–4(c). This proves that the energy acquirer retains a reliable operating mode under such complicated and large deformations. Furthermore, the currents produced when the device is attached to the wrist, elbow, and knee are 5, 13, and 20 nA, respectively. These values greatly exceed the current generated by a rigid functional module with low flexibility. Moreover, from the quantified consistent performance of the device, it can be concluded that the ultrasensitive piezoelectric sensor can precisely and repeatedly detect the complicated movements of different human body joints. The frequency and amplitude of the feedback current signal can be used to determine the corresponding frequencies and amplitudes of human body movements.

Figure 4(d) shows the response of the device when attached to clothes that swing owing to human body movements, leading to the deformation of the device and the generation of a stable output current of 15 nA. Because of the irregular swinging of the clothes, the output current signal clearly exhibits randomness. Finally, the device is fastened to a foot to observe the electric signal produced as a result of normal walking and running. As shown in Figs. 4(e)–4(f), a high output current on the order of 100 nA is generated mainly by the persistent loading of the human body weight on the device, which induces the strong deformation of the PVDF fibers. Figure 5 shows images taken during the evaluation of the ultrasensitive piezoelectric sensor

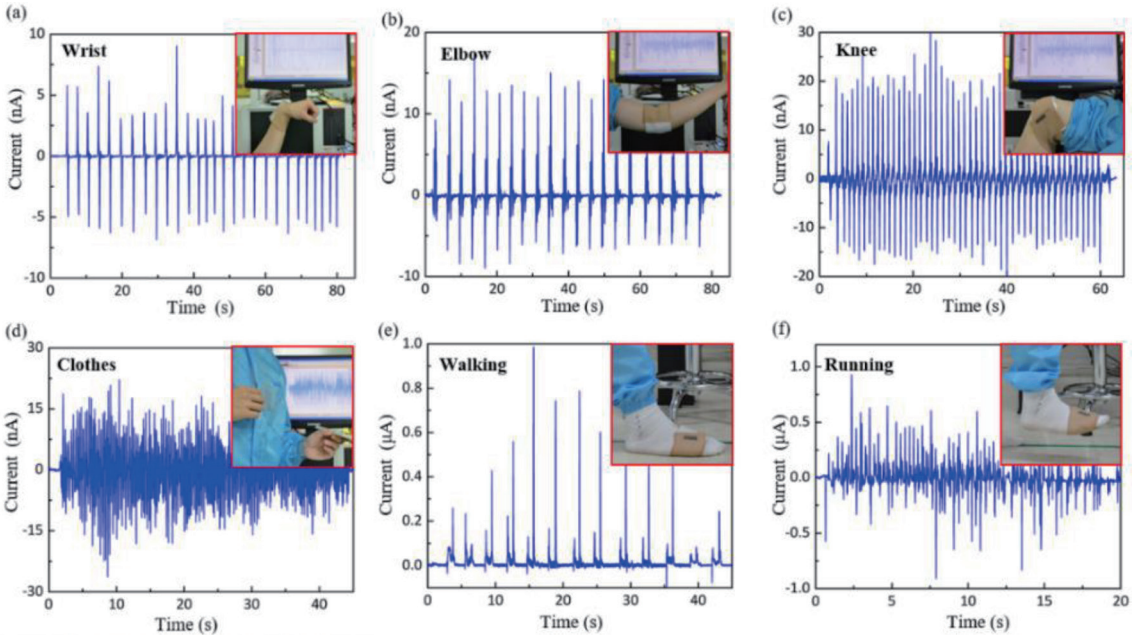

Fig. 4. (Color online) Piezoelectric properties of ultrastretchable sensor attached to (a) wrist, (b) elbow, (c) knee, (d) clothes, and (e, f) foot during (e) walking and (f) running.

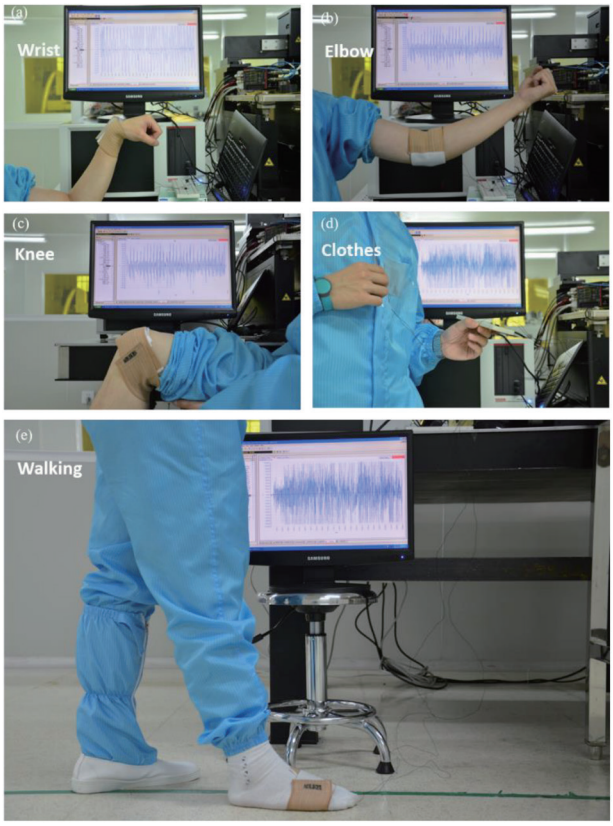

Fig. 5. (Color online) Images taken during evaluation of piezoelectric properties of ultrastretchable sensor attached to (a) wrist, (b) elbow, (c) knee, (d) clothes, and (e) foot during walking.

attached to various moving parts of the body. The device instantaneously converts mechanical energy as a result of a human body movement into an electric signal associated with the motion status, which can be used to identify details of the motion. This indicates the immense potential of such a device in actual applications. (The signal outputs of the sensor under different strains and other conditions are provided in Supplement C.)

The three sets of test results shown in Fig. 6 show the application of the piezoelectric sensor in human respiration and indoor detection. As shown in Fig. 6(a), the sensor at a distance of 20 cm from the nose can identify the status and intensity of respiration. If the device is attached near the philtrum, it may be possible to monitor the health state of the respiratory tract in real time. An early warning can significantly increase the likelihood of timely treatment of sudden illnesses such as a sudden onset of asthma at night. Figure 6(b) demonstrates that the sensor in a closed quiet room captures the airflow produced from a walking man up to a distance of 2.5 m. This suggests that the sensor can be used in safety and security systems.

3. Design and Testing of Flexible Piezoelectric OTFT Sensing System

The above performance test results clarify that the ultrastretchable piezoelectric sensor prepared using an electrohydrodynamic printing not only exhibits an excellent sensing ability

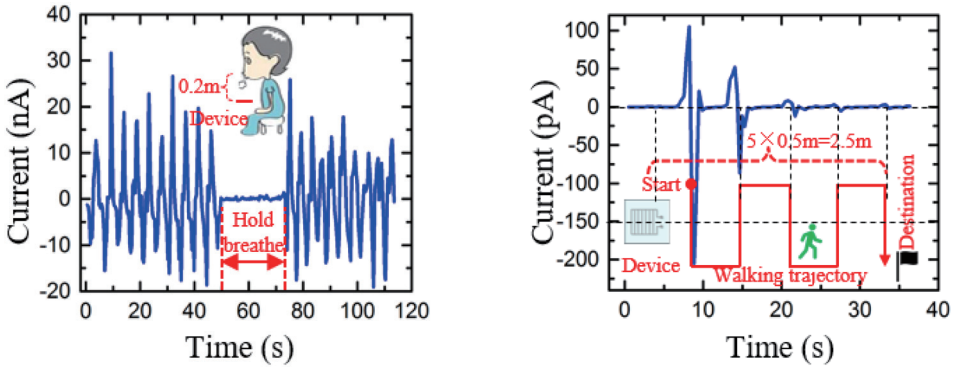

(a) (b)

Fig. 6. (Color online) (a) Electric response of ultrastretchable piezoelectric sensor to human respiration. (b) Electric response of ultrastretchable piezoelectric sensor to human walking away from sensor.

but also enables the sensing and monitoring of human body movements. However, in the exhibited applications, the electric tests still depended on commercial equipment such as a semiconductor tester, mainly because the current signal produced by the sensor is on the order of nA, which cannot be acquired effectively and simultaneously by common devices and chips. This imposes a large limitation on the practical application of sensors. Therefore, it is necessary to incorporate high-performance OTFT devices to effectively amplify the current signal. Additionally, the coordination between production and integration should also be given special consideration. Hence, we propose a flexible piezoelectric OTFT sensing system based on the microchannel OTFT prepared using an electrohydrodynamic direct-writing technology to promote the industrial-scale production of these sensors. (The fabrication of the thin-film transistor is described in Supplement A.)

An illustration of the as-prepared flexible piezoelectric OTFT sensing system is presented in Fig. 7(a). One end of the electrode of the ultrastretchable piezoelectric sensor is connected to the ground, while the other end is adhered to the bottom gate of a flexible OTFT through conductive silver paste, ensuring a relatively small contact resistance and excellent conduction. The source–drain electrodes of the OTFT are connected to an acquisition apparatus, such as an oscilloscope, by lead wires. The source electrode requires a small external voltage of ~3 V, which is provided temporarily by power from an external chip and hence not shown in Fig. 7. Since the OTFT is an active device actuated by voltage, the successful implementation of the system is dependent on the consistency between the output voltage signal and the operating voltage of the flexible OTFT. Figure 7(b) shows the output electric signal of the ultrastretchable piezoelectric sensor gripped in air under a stretching rate of 150% and a load offset of 12 mm. The current amplitude is approximately 80 nA and the voltage amplitude is approximately 300 mV. The output signal exhibits excellent repeatability. The large-area array with a linear structure and the micro–nanochannel structure obtained using a controllable electrohydrodynamic direct-writing technology are used to implement a flexible organic membrane-based single-gate transistor, whose transfer characteristic curve is presented in Fig. 7(c). From Fig. 7(c), it is not difficult to observe that the outperformance of the transistor is

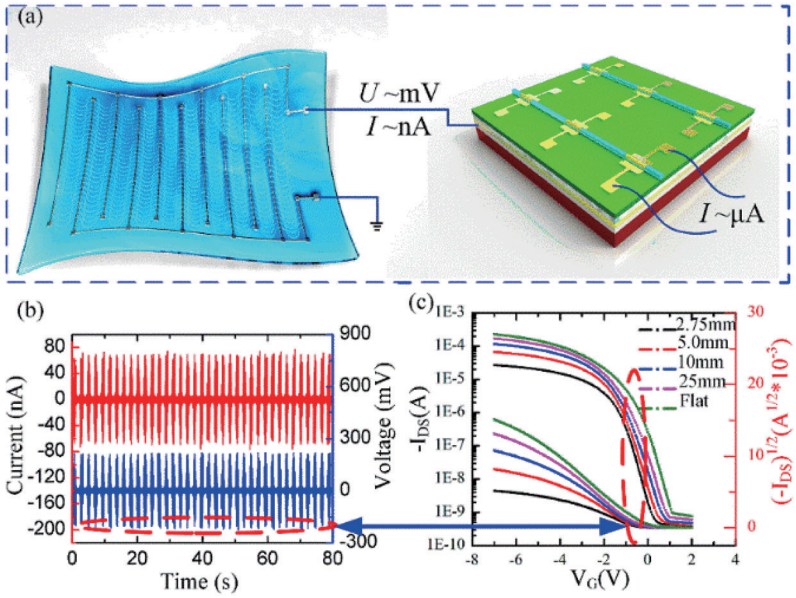

Fig. 7. (Color online) (a) Illustration of flexible piezoelectric OTFT sensing system. (b) Current–voltage output from ultrasensitive piezoelectric sensor. (c) Offset characteristic curve of flexible OTFT.

stable and reliable under different bending radii, which means that the transistor can adapt to the large strain on the body. The device should be equipped with the desired deformability to allow its attachment to a moving human body without affecting its operation. In addition, the threshold voltage of the OTFT is 0.8 V with a transconductance of 148 mV/dec. These values indicate the satisfactory discharge performance of the transistor under a relatively small grid voltage. According to Figs. 7(b) and 7(c), the output voltage of the piezoelectric sensor is roughly 300 mV, which, as the grid voltage of the OTFT, is sufficient for the actuation of the transistor to output a relatively large current signal. The output signal can be acquired in real time by an oscilloscope or IC chip. Thus, the proposed flexible sensing system is fundamentally feasible.

To evaluate the proposed flexible sensing system structure, the output current signal is first tested only for the ultrastretchable sensor gripped in air under a stretching rate of 150% and a load offset of 12 mm. As shown in Fig. 8(a), an output amplitude of only about 75 nA was acquired in real time by the semiconductor tester. Subsequently, the sensor was connected to the OTFT through lead wires and silver paste, as mentioned above. The load imposed on the sensor was unaltered, whereas the quantity detected by the semiconductor tester was the current between the source and drain electrodes of the OTFT, rather than the current between the electrodes of the piezoelectric sensor. The test results are shown in Fig. 8(b). It can be seen that the current signal of the OTFT is synchronous with the voltage signal and that the characteristic waveform of the negative voltage output is retained. Firstly, since the OTFT is regulated by the piezoelectric signal from the sensor as the grid voltage, the variation in the output current of the OTFT is consistent with the voltage. Secondly, the prepared OTFT is a p-type transistor. Therefore, the current increases sharply with a negative grid voltage, and a positive

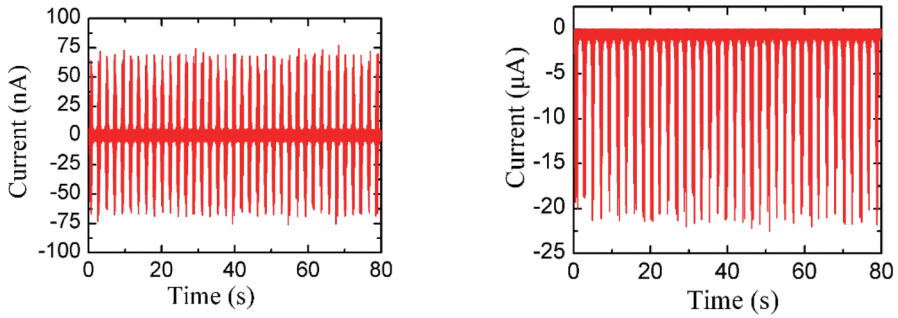

(a) (b)

Fig. 8. (Color online) (a) Current output signals from only ultrastretchable piezoelectric sensor. (b) Current output after amplification by flexible OTFT.

grid voltage switches the transistor off, producing a current on the order of pA, which can be neglected. Thus, the output current is similar to the piezoelectric signal after amplification and rectification. Even though some of the features of the waveform are lost, the weak current of 75 nA is amplified into a strong current output of 20 μA, corresponding to amplification by a factor of 260. Such a strong signal is sufficient for acquisition by traditional IC chips, marking significant progress toward the application of such ultrastretchable piezoelectric sensors.

The flexible piezoelectric OTFT sensing system with the sensor that has ultrasensitivity to human body movements can be directly attached to human bodies owing to the extremely high deformability of the sensor and the flexural ability of the OTFT. After detecting human body movements, the subsequently amplified output signal can be acquired and processed by a traditional chip, contributing to the practical application of the flexible piezoelectric system.

Figure 9(a) provides an actual view of the flexible piezoelectric OTFT sensing system attached to a wrist. The ultrasensitive piezoelectric sensor can be attached directly to human body joints such as wrists because of its ultrastretchability. Also, the movement of joints does not affect the sensitivity of the device. However, the limited flexural ability of the flexible OTFT array only allows attachment to surfaces such as an arm. Although only one OTFT of the OTFT array is used, it makes a significant contribution to piezoelectric sensors with an array configuration designed for a more elaborate detection such as that of the pressure distribution in an area of concern. The sensor and OTFT are connected by metal wires. During intense movements of the wrist, the stretching of Ecoflex actuates the internal PVDF fiber array with a self-similar structure, and thus the sensor produces a voltage–current output signal. Figure 9(b) shows the current signal from the piezoelectric sensor without the amplification of the signal by the OTFT. The current amplitude is within 5–10 nA. Owing to the random movement of the wrist, the stochastic amplitude and velocity lead to instability in the current signal, producing difficulties in signal acquisition and a high susceptibility to the submergence of the signal feature in ambient noise. The current output signal after amplification by the OTFT is presented in Fig. 9(c). The amplitude of the current signal is 2–5 μA, corresponding to an amplification factor of 500, as compared with that of the current signal in Fig. 9(b). The current signal of μA order is compatible with traditional chips for subsequent acquisition and processing.

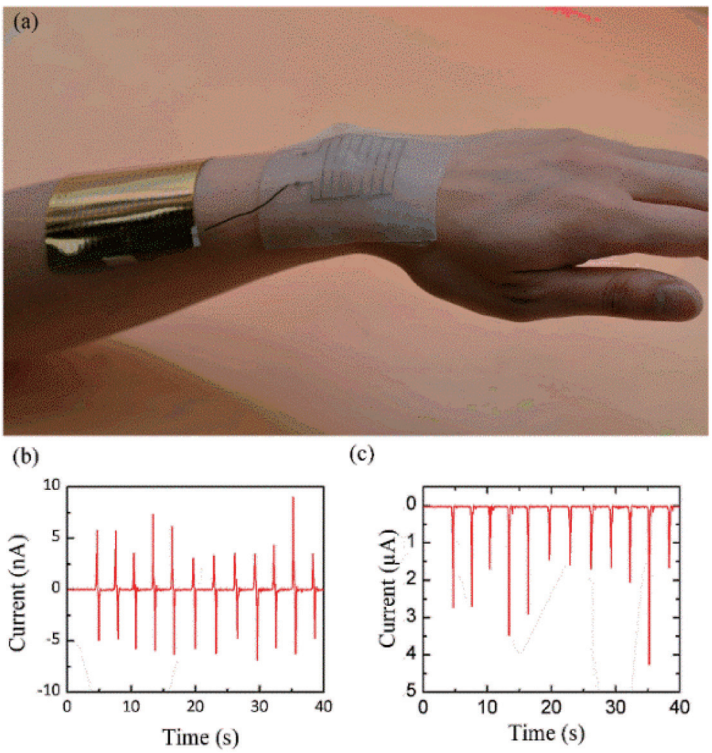

Fig. 9. (Color online) (a) Actual view of flexible piezoelectric OTFT sensing system attached to human body and current output signals of (b) sensor and (c) flexible piezoelectric OTFT sensing system in response to wrist movement.

Furthermore, the negative effects of ambient noise are reduced as the difference between feature signals is also amplified. This shows that the sensing system has an increased stability, but the signal features after amplification are partly lost. This can be addressed by replacing the semiconductor layer of the OTFT with bipolar function materials to give integrated signal data.

As a final verification of the reliability and applicability of the flexible piezoelectric OTFT sensing system, the piezoelectric sensor used in the above tests is substituted by the newly established flexible piezoelectric sensing system, and the current outputs for elbow movement, knee movement, the shaking of clothes, and walking were obtained, as shown in Fig. 10. Figure 10(a) presents the current signal as a result of repeated curling of the elbow with a continuously varying speed, where the current signal exhibits a larger amplitude at a higher speed. Similarly to Fig. 10(a), Fig. 10(b) shows the current signal for the repeated rebounding of the knee, whereas Fig. 10(c) shows the current signal obtained by shaking clothes at different speeds. The chaotic signal due to intense fluctuations makes it difficult to extract the effective signal. Figure 10(d) shows the current signal obtained when walking, first with increasing stride frequency and then with decreasing stride frequency. The detected signal clearly first displays an increase in current followed by a decrease because of its positive correlation with the stride frequency. This demonstrates the potential application of the sensing system for monitoring the stride frequency of human walking or running. By comparison with the current signal in Fig. 4, it

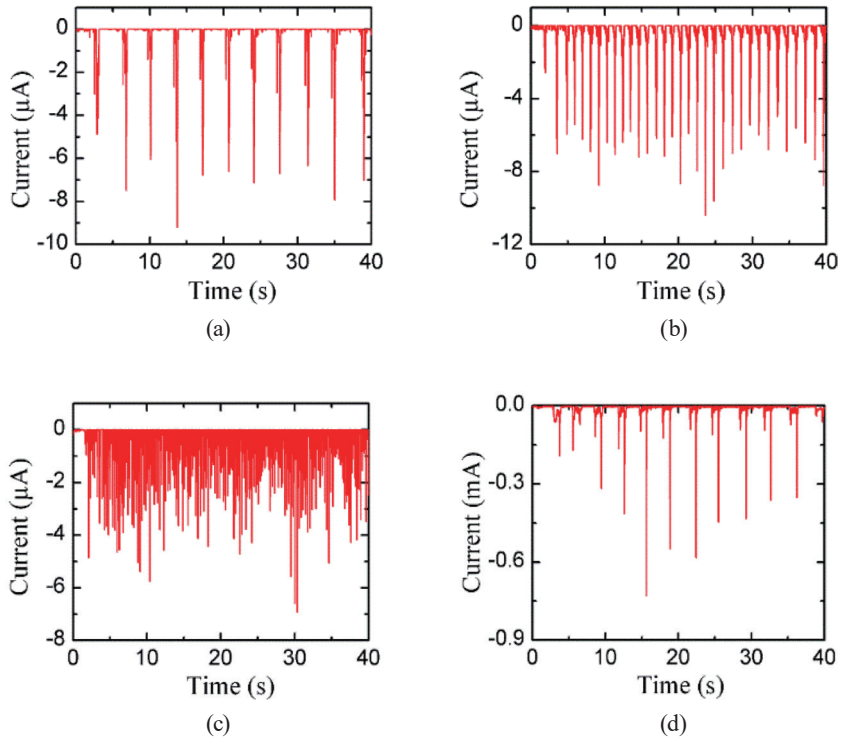

Fig. 10. (Color online) Current output signals from newly established flexible piezoelectric sensing system in response to detected human body movements: (a) elbow movement, (b) knee movement, (c) shaking of clothes, and (d) walking.

can be seen that the OTFT amplifies the signal by a factor of 300–1000. In the case of walking, the maximum current signal after amplification is up to 1 mA, showing the high amplifying performance of the OTFT. In summary, the established flexible piezoelectric sensing system can monitor human body movements effectively, and the output signal can be received directly by a traditional signal acquisition module, providing a solid basis for developing flexible wearable sensing systems.

4. Conclusion

In the current study, an electrohydrodynamic direct-writing technology, together with a flexible basal plate and a liquid metal, is used to prepare an ultrastretchable piezoelectric sensor, which is capable of handling large deformations. The ultrastretchable sensor is applied directly to monitor human body movements and respiration, and an output signal on the order of nA with regular variation corresponding to the movements and respiration is obtained. A flexible piezoelectric OTFT sensing system is established by coordinating the amplified signal from an OTFT and the sensor, where the original weak signal of nA order is amplified to μA or even mA order and can be received directly by a traditional acquisition circuit. The complete flexible piezoelectric sensing system was applied to sense human body movements with the current

signal amplified by the OTFT. These findings are a substantial contribution toward the practical application of ultrastretchable sensors and provide guidance for the manufacturing of wearable sensing devices.

References

1 D. Kim, N. Lu, Y. Huang, and J. Rogers: MRS Bull. **37** (2012) 226. https://doi.org/10.1557/mrs.2012.36
2 J. Rogers, T. Someya, and Y. Huang: Science **327** (2010) 1603. https://doi.org/10.1126/science.1182383
3 K. Fuh, Y. Chen, and C. Ye: Appl. Phys. Lett. **103** (2013) 033114. https://doi.org/10.1063/1.4813909
4 M. Park, J. Im, M. Shin, Y. Min, J. Park, H. Cho, S. Park, M.-B. Shim, S. Jeon, D.-Y. Chung, J. Bae, J. Park, U. Jeong, and K. Kim: Nat. Nanotechnol. **7** (2012) 803. https://doi.org/10.1038/nnano.2012.206
5 J. Viventi, D.-H. Kim, L. Vigeland, E. S. Frechette, J. A. Blanco, Y.-S. Kim, A. E. Avrin, V. R. Tiruvadi, S.-W. Hwang, A. C. Vanleer, D. F. Wulsin, K. Davis, C. E. Gelber, L. Palmer, J. Van der Spiegel, J. Wu, J. Xiao, Y. Huang, D. Contreras, J. A. Rogers, and B. Litt : Nat. Neurosci. **14** (2011) 1599. https://doi.org/10.1038/nn.2973
6 S. Park, D. S. Brenner, G. Shin, C. D. Morgan, B. A. Copits, H. U. Chung, M. Y. Pullen, K. N. Noh, S. Davidson, S. J. Oh, J. Yoon, K.-I. Jang, V. K. Samineni, M. Norman, J. G. Grajales-Reyes, S. K. Vogt, S. S. Sundaram, K. M. Wilson, J. S. Ha, R. Xu, T. Pan, Tae-il Kim, Y. Huang, M. C. Montana, J. P. Golden, M. R. Bruchas, R. W. Gereau IV, and J. A. Rogers: Nat. Biotechnol. **33** (2015) 1280. https://doi.org/10.1038/nbt.3415
7 H. Y. Kim; M. Lee, K. J. Park, S. Kim, and L. Mahadevan: Nano Lett. **10** (2010) 2138. https://doi.org/10.1021/nl100824d.
8 T. Huang, C. Wang, H. Yu, H. Z. Wang, Q. H. Zhang, and M. F. Zhu: Nano Energy **14** (2015) 226. https://doi.org/10.1016/j.nanoen.2015.01.038.
9 W. Zeng, X. M Tao, S. Chen, S. M. Shang, H. Chan, and S. H. Choy: Energy Environ. Sci. **6** (2013) 2631. https://doi.org/10.1039/c3ee41063c.
10 M. Habibi, J. Najafi, and N. M. Ribe: Phys. Rev. E. **84** (2011) 1. https://doi.org/10.1103/physreve.84.016219.
11 S. Ma, Q. Sun, Y. Su, R. Chen, and L. Wang: TELKOMNIKA **14** (2016) 145. https://doi.org/10.12928/TELKOMNIKA.v14i2A.4365.
12 Y. Q. Duan, Y. A. Huang, and Z. P. Yin: J. Phys. D: Appl. Phys. **48** (2015) 045302. https://doi.org/10.1088/0022-3727/48/4/045302.
13 X. Chen, M. Han, H. Chen, X. Cheng, Y. Song, Z Su, Y. Jiang, and H. Zhang: Nanoscale **9** (2017) 1263. https://doi.org/10.1039/c6nr07781a.
14 M. Kaltenbrunner, T. Sekitani, J. Reeder, T. Yokota, K. Kuribara, T. Tokuhara, M. Drack, R. Schwodiauer, I. Graz, S. Bauer-Gogonea, S. Bauer, and T. Someya: Nature **499** (2013) 458. https://doi.org/10.1038/nature12314.
15 T. Someya, Y. Kato, T. Sekitani, S. Iba, Y. Noguchi, Y. Murase, H. Kawaguchi, and T. Sakurai: Proc. Natl. Acad. Sci. U.S.A. **102** (2005) 12321. https://doi.org/10.1073/pnas.0502392102.
16 T. Someya, T.Sekitani, S. Iba, Y. Kato, H. Kawaguchi, and T. Sakurai: Proc. Natl. Acad. Sci. U.S.A. **101** (2004) 9966. https://doi.org/10.1073/pnas.0401918101.
17 C. Dagdeviren, Y. Su, P. Joe, R. Yona, Y. Liu, Y. S. Kim, Y. Huang, A. R. Damadoran, J. Xia, L. W. Martin, Y. Huang, and J. A. Rogers: Nat. Commun. **5** (2014) 4496. https://doi.org/10.1038/ncomms5496.
18 T. Yokota, Y. Inoue, Y. Terakawa, J. Reeder, M. Kaltenbrunner, T. Ware, K. Yang, K. Mabuchi, T. Murakawa, M. Sekino, W. Voit, T. Sekitani, and T. Someya: Proc. Natl. Acad. Sci. U.S.A. **112** (2015) 14533. https://doi.org/10.1073/pnas.1515650112.